

Using the Intensity Modulation Index to Test Pulsar Radio Emission Models

Fredrick A. Jenet ¹, Janusz Gil²

ABSTRACT

This letter explores the possibility of testing pulsar radio emission models by observing pulse-to-pulse intensity modulation. It is shown that a relationship between a pulsar's period, period derivative, and intensity modulation is a natural consequence of at least one theoretical model of radio pulsar emission. It is proposed that other models may also predict a similar correlation. The exact form of the relationship will depend on the model in question. Hence, observations of intensity modulation should be able to determine the validity of the various emission models. In an attempt to search for the predicted dependencies, the modulation properties of a set of 12 pulsars are studied. These data are suggestive, but they are unable to differentiate between three possibilities for the emission process. Future observations will be able to confirm these results and determine whether or not specific emission models are viable.

Subject headings: pulsars:general

1. Introduction

The cause of the emission from radio pulsars has remained elusive since their discovery over 30 years ago. The high brightness temperature together with the enormous amount of phenomenology exhibited make these sources very difficult to understand. This letter focuses on pulse-to-pulse fluctuations and it will describe how they may be used to test emission models.

Observations of bright pulsars have shown that the shapes and intensities of individual pulses are unique, although they average together to form a stable mean profile. The characteristic widths of individual pulses, typically referred to as sub-pulses, are usually smaller

¹California Institute of Technology, Jet Propulsion Laboratory
4800 Oak Grove Drive, Pasadena, CA 91109

²Institute of Astronomy, University of Zielona Góra
Lubuska 2, 65-265, Zielona Góra, Poland

than the average profile width. Some pulsars show rapid intensity fluctuations or microstructure. The time scales of these fluctuations vary from source to source and they range from 1 ms down to 2 ns (Hankins et al. 2003).

Recent observations of PSR B1937+21 show a behavior that is completely different from previously studied sources (Jenet et al. 2001, J01 hereafter). This source exhibits no detectable pulse-to-pulse fluctuations. Occasional bursts of radio radiation, or “Giant pulses”, are observed but they are restricted to small regions in pulse phase (Kinkhabwala & Thorsett 2000; Cognard et al. 1996). Understanding what makes the non-giant pulse emission of PSR B1937+21 so unique will help us to understand the radio emission process. The possibility that this steady behavior is just an extreme case of a general phenomenon is explored in this letter.

The ideas presented here will be focused on the modulation index, which is a measure of pulse-to-pulse intensity fluctuations. The modulation index is known to be a function of pulsar pulse phase, hence one may define a phase resolved modulation index as follows:

$$m(\phi) = \frac{\sqrt{\langle I(\phi)^2 \rangle - \langle I(\phi) \rangle^2}}{\langle I(\phi) \rangle}, \quad (1)$$

where m is the modulation index, ϕ is the pulse phase, I is the pulsar intensity, and the angle brackets represent averaging over a large ensemble of adjacent pulses. Recent theoretical work by Gil & Sendyk (2000, GS00 henceforth) suggests that the pulsar intensity modulation index should depend on some function of the pulsar period (P) and period derivative (\dot{P}). The exact functional dependence will depend on the region of pulse phase being studied. More specifically, it will depend on whether the phase region is classified as a “core” or “conal” component as defined by Rankin (1983, 1986). Due to current constraints on the available data and the predictions of the GS00 model, the work here will focus on core component emission only.

The GS00 model is based on the polar cap spark model of Ruderman & Sutherland (1975). Both of these models have received much attention in recent years. They have been used to interpret the sub-pulse properties of slow pulsar conal emission (Edwards, Stappers, & van Leeuwen 2003; Rankin & Ramachandran 2003; van Leeuwen, Stappers, Ramachandran, & Rankin 2003; Asgekar & Deshpande 2001; Deshpande & Rankin 2001) and of millisecond pulsar core emission (Edwards & Stappers 2003). These models have also been used in pulsar population studies (Arzoumanian, Chernoff, & Cordes 2002; Fan, Cheng, & Manchester 2001).

In general, a given theory of the emission physics should be able to make quantitative predictions for the dependence of m on P and \dot{P} . Observations should then be able to

rule out various classes of models. The predictions of the GS00 model together with other possible models are discussed in section 2. Section 3 demonstrates how these models can be tested. This letter is summarized in section 4.

2. Models of Intensity Modulation

It is generally accepted that the observed pulsar radio emission is generated within a dense electron-positron plasma flowing along the open magnetic field lines of the neutron star. Open field lines are those that connect with the interstellar magnetic field rather than connecting back to the pulsar’s surface magnetic field. Intrinsic pulse-to-pulse intensity modulations can arise from the time-dependent lateral structure of this flow, probed once per pulsar period by the observer’s line-of-sight.

Ruderman & Sutherland (1975) proposed a pulsar model where bursts of plasma, or “sparks”, are generated at the polar cap. The electron-positron plasma created by a spark travels up along the magnetic field lines where it eventually emits radio radiation generated by some kind of instability (Asseo & Melikidze 1998; Melikidze, Gil & Pataraya 2000). GS00 explored the Ruderman & Sutherland model further in an attempt to describe pulsar radiation properties as a function of basic observable parameters such as P and \dot{P} . They postulated that the polar cap is populated as densely as possible with a number of these sparks, each having a characteristic size and separation from adjacent sparks that is approximately equal to the gap height h . This leads directly to the so called “complexity parameter” $a_1 = r_p/h$, equal to the ratio of the polar cap radius, r_p , to the characteristic spark dimension, h . Making a reasonable assumption about the non-dipolar surface magnetic field, GS00 found that

$$a_1 = 5(\dot{P}/10^{-15})^{2/7}(P/1s)^{-9/14}. \quad (2)$$

One can show that a_1 is the maximum number of sparks across the polar cap. It is also the maximum number of subpulses and/or profile components. Thus, a_1 describes the complexity of the mean pulse profile (see GS00 for details). Within a given polar cap region (i.e. core or conal region), the amplitude of the emitted radio radiation is roughly the same for each spark. Since each individual spark emits nearly steady, unmodulated radiation, the observed pulse-to-pulse fluctuations are due to the presence of several sparks moving either erratically or in an organized manner and emitting into the observers line of sight. As the number of sparks increases, one will expect to see less and less pulse-to-pulse intensity fluctuation. Hence, the modulation index should be anti-correlated to the complexity parameter in both core and conal components. Unfortunately, other effects such as those associated with viewing angle will mask this anti-correlation in the conal emission. Thus, the core emission is the most

direct way to observe this effect.

The GS00 model is based on instabilities in the polar cap plasma generation. There are several other magnetospheric instabilities that could, in principle, produce something like a complexity parameter that would be correlated to the modulation index. Three such instabilities are: continuous current outflow instabilities (Arons & Scharlemann 1979; Hirschman & Arons 2001), surface magnetohydrodynamic wave instabilities (Lou 2001) and possibly outer magnetospheric instabilities. Even though a complexity parameter has not been rigorously calculated for these models, one can estimate that the following parameters:

$$a_2 = \sqrt{\frac{\dot{P}}{P^3}}, \quad a_3 = \sqrt{P\dot{P}}, \quad a_4 = \sqrt{\frac{\dot{P}}{P^5}}, \quad (3)$$

would correspond to the complexity-like parameters for the current outflow, surface MHD wave, and outer magnetospheric instabilities, respectively. Physically, these parameters are proportional to the total current outflow from the polar cap, the surface magnetic field, and the magnetic field at the light-cylinder, respectively.

3. Analyzing the Intensity Modulation Properties

A comparison between the observed modulation indices of 12 pulsars and the various complexity parameters defined above is performed in this section. Data were obtained for 8 sources from Weisberg et al. (1986, W86 hereafter), 2 from J01, and 2 from recent data taken at the Arecibo Observatory using the Caltech Baseband Recorder. These sources are listed in Table 1 along with the measured modulation indices, observing frequencies, and references.

This study is focused on the emission properties of core components since the current form of the GS00 model is more directly applicable to core type emission. In general, the modulation indices of core type emission are lower than that of conal emission (W86). This effect is also a consequence of the GS00 model. For the case of multiple component profiles, if conal emission overlaps with core emission, the observed modulation index will be larger than that of the core emission alone. Even pulsars that are classified as primarily core emitters can have some conal emission near the edges of the profile (see § 5.4 in GS00). In order to reduce the effects of overlapping emission regions, the minimum value of the modulation index was chosen for each source. This will result in the best possible measurement of the core component’s modulation index.

Since the data from J01 were reported using a definition of the modulation index that included radiometer noise, the values were transformed in order to be consistent with the

definition in W86. The following transformation was applied (see J01 for details):

$$m = \sqrt{(m_j^2 - 1)/2}, \quad (4)$$

where m is the modulation index used in W86 as well as in this letter and m_j is the modulation index used in J01.

The measured modulation index depends on both intrinsic pulsar intensity fluctuations as well as fluctuations due to propagation through the interstellar medium (ISM). The functional form of this dependence is as follows:

$$m^2 + 1 = (m_i^2 + 1)(m_{ISM}^2 + 1), \quad (5)$$

where m , m_i and m_{ISM} are the measured, intrinsic, and ISM induced modulation indices, respectively. m_{ISM} may be estimated using the following relationship (Cordes et al. 1990):

$$m_{ISM} = 1/\sqrt{S}, \quad (6)$$

where S is the number of “scintills” in the receiver bandwidth. S is given by

$$S = 1 + \eta \frac{B}{\delta\nu}, \quad (7)$$

where B is the receiver bandwidth, $\delta\nu$ is the ISM decorrelation bandwidth, and η is a filling factor which ranges from 0.1 to 0.2. For each source, $\delta\nu$ was taken from Cordes (1986), η was set to 0.18, and the intrinsic modulation index was estimated using Equation 5. Note that the results presented here are insensitive to variations in η when this parameter is within the expected range. The adopted value of η was chosen so that each inferred intrinsic modulation index was non-zero.

Three criteria were used to select the sources used in this study. First, a given source had to have a measured period derivative (Taylor et al. 1993). Second, the ISM decorrelation bandwidth must be known (Cordes 1986). Third, the source had to have a core emission component.

In order to determine if any of the complexity parameters are correlated with the measured modulation indices, the Spearman Rank-Order Correlation (SROC) coefficient, ρ , and its associated significance parameter, Δ , are calculated between m and each a_i . Δ is simply the probability that such a correlation would occur in randomly distributed data. Hence, the smaller the value of Δ , the more significant the correlation. The SROC coefficient was chosen over other possible statistics for two reasons. First, it is more robust and conservative than the standard linear correlation coefficient (see §14.6 of Press et al. (1992)). Second, since it is a rank ordering method, $|\rho|$ and Δ are exactly the same for both the original data, (x_j, y_j) ,

and for $(F(x_j), G(y_j))$ where F and G are arbitrary, monotonic functions. This property is extremely useful since the current form of the GS00 model only predicts the existence of a relationship between m and a_1 rather than specifying an exact form.

Plots of m versus a_1 , a_2 , a_3 , and a_4 are shown in Figure 1. The error bars shown were taken to be the greater of the measurement uncertainty or the uncertainty due to the fact that η is unknown and can range from 0.1 to 0.2. The SROC coefficient, ρ , and the significance parameter, Δ , were calculated for the data, given each of the models. The results are tabulated in Table 2. ρ and Δ were calculated both with and without the ISM correction applied. For the sake of comparison, the correlation of m with P and with \dot{P} were calculated and included in the table. The sparking gap model a_1 of GS00 shows the best correlation, although a_2 and a_4 cannot be excluded.

The above analysis calculated the correlation between the intensity modulation index and four physically motivated parameters. An alternative to this approach is to calculate the correlation between m and a set of parameters given by the following one-dimensional family:

$$a(\alpha) = P^\alpha \dot{P}. \quad (8)$$

One can then find that α which maximizes both the absolute value of the correlation and its significance. This is equivalent to minimizing the significance parameter since Δ is a monotonic function of $|\rho|$. A range of admissible α values about this minimum can be obtained by choosing a threshold value of Δ . Since the SROC analysis is independent of an arbitrary monotonic function, it is not necessary to search over the two dimensional family of the form $P^\beta \dot{P}^\gamma$. For the data presented in Table 1 together with a threshold significance parameter of 1×10^{-3} , α ranged from -5.0 to -2.0 with a local minimum located at -2.7 . The minimum Δ was 2.8×10^{-5} and the corresponding correlation coefficient was -0.92 . The range of α values searched over was $[-100, 100]$ with a grid spacing of 0.01. $\Delta(\alpha)$ varies in a piece-wise continuous manner with only one local minimum that is also the global minimum in the region searched.

In order to determine the significance of the value of α found using the method described above, Monte-Carlo techniques were used to determine the probability of obtaining an α with $\Delta \leq 2.8 \times 10^{-5}$. For the same set of pulsars used above, random modulation indices were calculated and the minimum significance was found over a range of α values equal to $[-20, 20]$. Note that this range is smaller than that used above in order to reduce computation time. The grid spacing used here was also 0.01. When the modulation indices are chosen from a uniform distribution ranging from 0 to 1, the probability of obtaining $\Delta \leq 2.8 \times 10^{-5}$ is $.0011 \pm 9\%$. A random set of m values may also be obtained by randomly shuffling the measured set of modulation indices. When this is done, the probability becomes $.00074 \pm 12\%$.

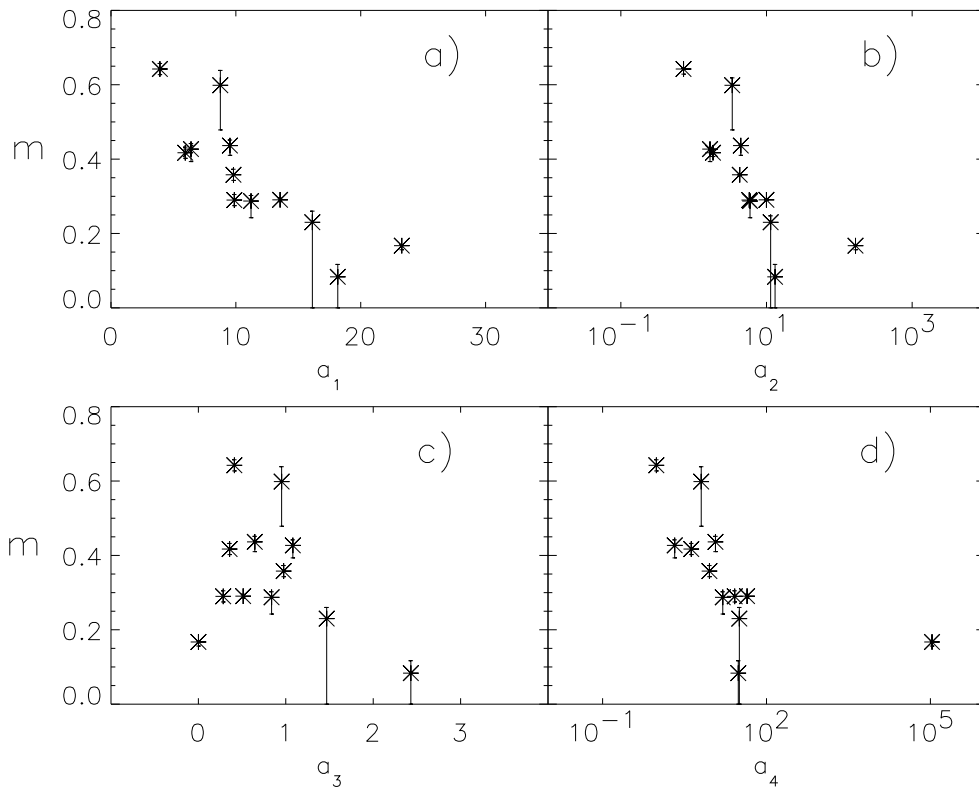


Fig. 1.— m versus different “complexity parameters”. These parameters are defined in Table 2. A log scale was used when the parameter varied over several orders of magnitude.

Table 1. Sources used in this analysis

Source (B1950)	m	Frequency (MHz)	Reference
0626+24	0.36 ± 0.015	430	W
0823+26	0.88 ± 0.04	430	J
0919+06	0.29 ± 0.015	430	W
1737+13	0.47 ± 0.015	430	W
1821+05	0.66 ± 0.015	430	W
1839+09	0.47 ± 0.015	430	W
1842+14	0.34 ± 0.015	430	W
1929+10	1.08 ± 0.005	1410	N
1933+16	0.38 ± 0.03	1666	N
2053+36	0.29 ± 0.015	430	W
2113+14	0.43 ± 0.015	430	W
1937+21	0.17 ± 0.003	430	J

References. — W = (Weisberg et al. 1986), J=(Jenet et al. 2001), N=this paper

Table 2. The Spearman rank-ordered correlation coefficients for several emission models

Parameter	Model Type	Definition	$\rho(\Delta)$	$\rho(\Delta)$ w/o ISM correction
a_1	Sparking Gap	$5(\dot{P})^{2/7} P^{-9/14}$	$-0.91(4 \times 10^{-5})$	$-0.59(0.04)$
a_2	Beam Instability	$\dot{P}^{1/2} P^{-3/2}$	$-0.90(1 \times 10^{-4})$	$-0.58(0.05)$
a_3	MHD Waves	$\dot{P}^{1/2} P^{1/2}$	$-0.13(0.68)$	$0.09(0.78)$
a_4	Instabilities at LC	$\dot{P}^{1/2} P^{-5/2}$	$-0.82(1 \times 10^{-3})$	$-0.45(0.14)$
		P	$0.69(0.01)$	$0.49(0.10)$
		\dot{P}	$-0.34(0.28)$	$-0.08(0.81)$

Note. — The Spearman Rank-Ordered Correlation coefficient, ρ , and its significance, Δ , are calculated between the modulation index, m , and the complexity parameters associated with four different emission models. For the sake of comparison, the table also lists the correlation between m and both P and \dot{P} . For all cases, P is in seconds and \dot{P} is in $10^{-15} s/s$. The correlations were calculated both with and without the interstellar medium correction applied. Δ is the probability of obtaining this correlation in random data.

4. Discussion & Summary

The set of 12 pulsars studied here suggests a relationship between the intensity modulation index, the pulsar period, and the period derivative. Future observations are needed in order to confirm this correlation. The search for such a relationship is an extremely powerful way to constrain emission mechanisms. Using “reasonable” assumptions about the pulsar magnetospheric plasma, the sparking gap model predicts a functional relationship between the modulation index, the period, and the period derivative. If this correlation is shown not to exist, then the assumptions, and perhaps the entire model, are incorrect. The same may hold true for the other models discussed here, if it can be shown that such correlations should exist. On the other hand, if the correlation seen here is confirmed, then the exact functional relationship will be able to determine which model, if any, is the most likely candidate. The current data supports complexity parameters of the form given by Equation 8 with α between -5.0 and -2.0 . Among the physical models presented, the sparking gap model, a_1 ($\alpha = -2.25$), shows the highest correlation, although the beam current model, a_2 ($\alpha = -3.0$), and the light cylinder model, a_4 ($\alpha = -5.0$), cannot be ruled out. The surface MHD wave model, a_3 ($\alpha = 1.0$), is unlikely. The minimization analysis favors $\alpha = -2.7$ but the corresponding values of ρ and Δ are only slightly better than those found for the sparking gap model. If follow-up observations confirm that $\alpha = -2.7$, then none of the above models fully capture the physics of the emission process.

Future observations will provide a data set far superior to the one used in this analysis. Using the statistical techniques employed by J01, the modulation indices of a much larger sample of pulsars can be measured. Also, the ISM parameters, η and $\delta\nu$, which are known to vary with time, can be measured simultaneously with the modulation index. This will enable a more accurate determination of the intrinsic modulation index. Note that for this work, η was assumed to be 0.18 for all sources and the decorrelation bandwidths were taken from previously published results.

It should be noted that recent work on the Vela pulsar shows that this source exhibits large pulse-to-pulse modulation (Kramer et al. 2002). In each of the supported models, this source should have almost no modulation. Since this pulsar is classified as a core emitter, it will be an exception to the work presented here. If future observations confirm the above correlation, then this source may be understood within the framework of the supported models. For example, in the context of the sparking gap model this pulsar may have surface magnetic field structures or relativistic plasma γ factors which differ significantly from the main group. It is also possible that Vela may belong to a class of pulsars which obey a different m , P , and \dot{P} relationship.

The ideas presented here were motivated by observations of PSR B1937+21 in which

no detectable pulse-to-pulse modulation was found. In the context of each of the models discussed above, the stability of this pulsar’s emission would be a consequence of its relatively high complexity parameter. The physical reason for the stability will be constrained further when future observations confirm the correlation discussed here and determine its functional form more accurately.

In summary, the relationship between a pulsar’s pulse-to-pulse intensity fluctuations, period, and period derivative will provide a valuable insight into the physical processes responsible for the radio emission. Such a relationship could offer a simple explanation for the unique behavior observed in PSR B1937+21. The data presented in this letter supports such a relationship although future observations are needed in order to confirm its existence.

This paper is supported in part by the grant 2 P03D 008 19 of the Polish State Committee for scientific research. Part of this research was performed at the Jet Propulsion Laboratory, California Institute of Technology, under contract with the National Aeronautics and Space Administration. The authors wish to thank John Armstrong and Linqing Wen for useful discussions, Stuart Anderson for helping to take the data, and the anonymous referee who made several useful suggestions. Special thanks goes to E. B. Dussan V. and Thomas A. Prince.

REFERENCES

- Arons, J., & Scharlemann, E. T., ApJ, 231, 854
- Arzoumanian, Z., Chernoff, D. F., & Cordes, J. M. 2002, ApJ, 568, 289
- Asseo, E., & Melikidze, G.I., 1998, MNRAS 301, 59
- Asgekar, A. & Deshpande, A. A. 2001, MNRAS, 326, 1249
- Cognard, I., Shrauner, J. A., Taylor, J. H., & Thorsett, S.E. 1996, ApJ,457,L81
- Cordes, J. M. 1986, ApJ, 331, 183
- Cordes, J. M., Wolszczan, A., Dewey, R. J., Blaskiewicz, M., & Stinebring, D. R. 1990, ApJ, 349, 245
- Deshpande, A. A. & Rankin, J. M. 2001, MNRAS, 322, 438
- Deshpande, A. A., & Rankin, J. M. 1999, ApJ, 524, 1008

- Edwards, R. T., & Stappers, B.W., astro-ph/0305266, in press
- Edwards, R. T., Stappers, B. W., & van Leeuwen, A. G. J. 2003, *A&A*, 402, 321
- Fan, G. L., Cheng, K. S., & Manchester, R. N. 2001, *ApJ*, 557, 297
- Gil, J., & Sendyk, M. 2000, *ApJ*, 541, 351 (GS00) U., 2003, *A&A*, 407,315
- Hankins, T. H., Kern, J. S., Weatherall, J. C., & Eilek, J. A. 2003, *Nature*, 422, 141
- Hibschman, J. A., & Arons, J. 2001, *ApJ*, 560, 871
- Jenet, F., Anderson, S. B., & Prince, T.A. 2001, *ApJ*, 546, 394 (J01)
- Kinkhabwala, A. & Thorsett, S. E. 2000, *ApJ*, 535, 365
- Kramer, M., Johnston, S., & van Straten, W. 2002, *MNRAS*, 334, 523
- Lou, Y. 2001, *ApJ*, 563, 147
- Melikidze, G.I., Gil, J. & Pataraya, A.D., 2000, *ApJ*, 544, 1081
- Press, W. H., Teukolsky, S. A., Vetterling, W. T., & Flannery, B. P. 1992,
Numerical Recipes in C (2nd ed.; Cambridge: University Press)
- Rankin J. M., 1983, *ApJ*, 274, 333
- Rankin J. M., 1986, *ApJ*, 301, 901
- Rankin, J. M. & Ramachandran, R. 2003, *ApJ*, 590, 411
- Ruderman, M. A., & Sutherland, P. G. 1975, *ApJ*, 196,51 (RS75)
- Taylor, J. H., Manchester, R. N., & Lyne, A. G. 1993, *ApJS*, 88, 529
- van Leeuwen, A. G. J., Stappers, B. W., Ramachandran, R., & Rankin, J. M. 2003, *A&A*,
399, 223
- Weisberg, J. M., Armstrong, B. K., Backus, P. R., et al. 1986, *AJ*, 92, 621 (W86)